

1 **Bacteriostatic antibiotics promote the evolution of CRISPR-Cas immunity**

2

3 Tatiana Dimitriu^{1*}, Elena Kurilovich², Urszula Lapinska³, Konstantin Severinov^{2,4,5}, Stefano

4 Pagliara³, Mark D. Szczelkun⁶, Edze R. Westra^{1*}

5 ¹ ESI, Biosciences, University of Exeter, TR10 9FE Penryn, UK

6 ² Center of Life Sciences, Skolkovo Institute of Science and Technology, Moscow 143028,

7 Russia

8 ³ Living Systems Institute, Biosciences, University of Exeter, EX4 4QD Exeter, UK

9 ⁴ Waksman Institute of Microbiology, Piscataway, NJ 08854, USA

10 ⁵ Institute of Molecular Genetics, Russian Academy of Sciences, Moscow 119334, Russia

11 ⁶ DNA-Protein Interactions Unit, School of Biochemistry, University of Bristol, BS8 1TD,

12 Bristol, UK

13 * e-mail: T.Dimitriu@exeter.ac.uk; E.R.Westra@exeter.ac.uk

14

15

16 **Abstract**

17

18 Phage therapy can be used in combination with antibiotics to combat infections with bacterial
19 pathogens¹⁻³. However, bacteria can rapidly evolve phage resistance via receptor mutation, or
20 using their CRISPR-Cas adaptive immune systems⁴, which insert short phage-derived
21 sequences into CRISPR loci in the bacterial genome⁵ to guide sequence-specific cleavage of
22 cognate sequences⁶. Unlike CRISPR-Cas immunity, mutation of the phage receptor leads to
23 attenuated virulence when the opportunistic pathogen *Pseudomonas aeruginosa* is infected
24 with its phage DMS3vir⁷, which underscores the need to predict how phage resistance evolves
25 under clinically relevant conditions. Here, using eight antibiotics with various modes of action,
26 we show that bacteriostatic antibiotics (which inhibit cell growth without killing) specifically
27 promote evolution of CRISPR-Cas immunity in *P. aeruginosa* by slowing down phage
28 development and providing more time for cells to acquire phage-derived sequences and mount
29 an immune response. Our data show that some antimicrobial treatments can contribute to the
30 evolution of phage-resistant pathogens with high virulence.

31

32 **Main text**

33

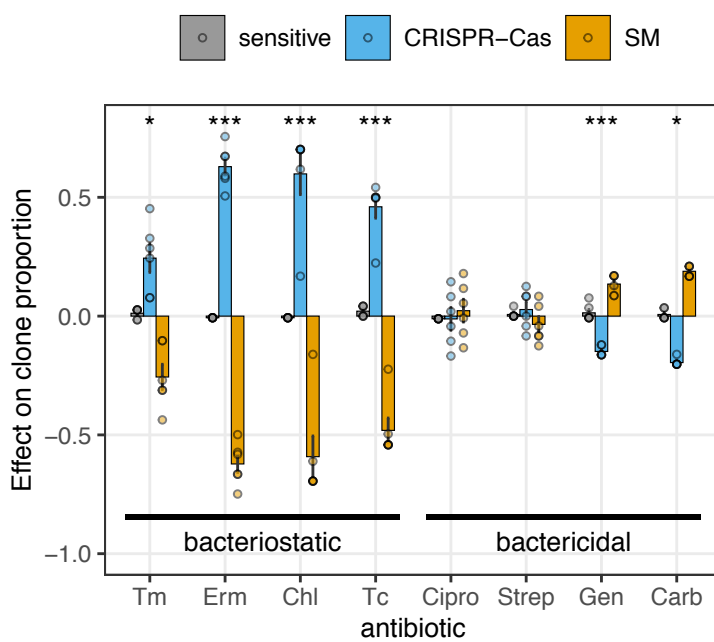
34 We studied the effect of antibiotics on the evolution of CRISPR-Cas immunity in *Pseudomonas*
35 *aeruginosa*, an opportunistic pathogen that commonly evolves antibiotic resistance and that
36 has elicited large interest in phage and phage-antibiotic combination therapies for treatment of
37 *P. aeruginosa* infections⁸⁻¹⁰. *Pseudomonas* strain PA14 can acquire immunity against its lytic
38 phage DMS3vir¹¹ by acquiring phage sequences (spacers) into CRISPR loci in its genome¹².
39 However, despite the presence of an active CRISPR-Cas system, this bacterium mostly evolves
40 resistance through surface modification (SM) by loss or mutation of the type IV pilus
41 (DMS3vir receptor) in rich broth and in artificial sputum medium that mimics the cystic
42 fibrosis lung environment it commonly colonizes^{7,13}.

43

44 ***Antibiotics effects on phage resistance***

45 To understand how antibiotics shape the population and evolutionary dynamics of *P.*
46 *aeruginosa* during phage infection, we infected PA14 cultures grown in rich medium
47 supplemented with sub-inhibitory concentrations of 8 different antibiotics (Extended Data Fig.
48 1A) with phage DMS3vir. Of these antibiotics, four are bactericidal (ciprofloxacin (Cipro),
49 streptomycin (Strep), gentamycin (Gen) and carbenicillin (Carb)) and four are bacteriostatic
50 (chloramphenicol (Chl), tetracycline (Tc) erythromycin (Erm), and trimethoprim (Tm)) against
51 *P. aeruginosa* (Extended Data Fig. 1B). Most antibiotics delayed the phage epidemics and
52 subsequently the evolution of phage resistance (Extended Data Fig. 2A and B). Nonetheless,
53 at 3 days post infection (d.p.i.) phage resistance was essentially fixed in all cultures (Extended
54 Data Fig. 2C). Strikingly, at this point, the type of phage resistance that had evolved was
55 strongly dependent on the presence and the type of antibiotic. In the absence of antibiotics, or
56 in the presence of bactericidal antibiotics, only a minority of bacteria evolved CRISPR-Cas

57 immunity¹³, whereas a large proportion of the bacterial population evolved CRISPR-Cas
58 immunity in the presence of bacteriostatic antibiotics (Fig. 1 and Extended Data Fig. 2D). This
59 effect was relatively weak for Tm compared to Tc, Erm and Chl (Fig. 1). Chl was found to
60 trigger CRISPR immunity across a wide range of concentrations, whereas no effect was
61 observed when we used a Chl-resistant strain (Extended Data Fig. 3A). These data, and the fact
62 that Chl, Tc, Erm and Tm have different modes of action, suggests that bacteriostatic antibiotics
63 promote evolution of CRISPR immunity because they limit bacterial growth rates.



64
65 **Figure 1: Bacteriostatic antibiotics promote CRISPR-Cas immunity.** Effect of antibiotics
66 on the proportion of sensitive (grey), CRISPR-Cas (blue) and SM clones (yellow) at 3 d.p.i.,
67 compared to the associated no-antibiotic treatment. Bars and error bars show mean \pm s.e.m.,
68 and individual biological replicates are plotted as dots (N=6). Asterisks indicate antibiotics
69 with CRISPR-Cas proportion significantly different from the associated no-antibiotic treatment
70 (* $0.01 < p < 0.05$; *** $p < 0.001$). Antibiotics are ordered from left to right by decreasing
71 minimum bactericidal concentration / minimum inhibitory concentration ratio, a measure of
72 their bacteriostatic vs bactericidal activity. Raw data are shown in Extended Data Fig. 2D.

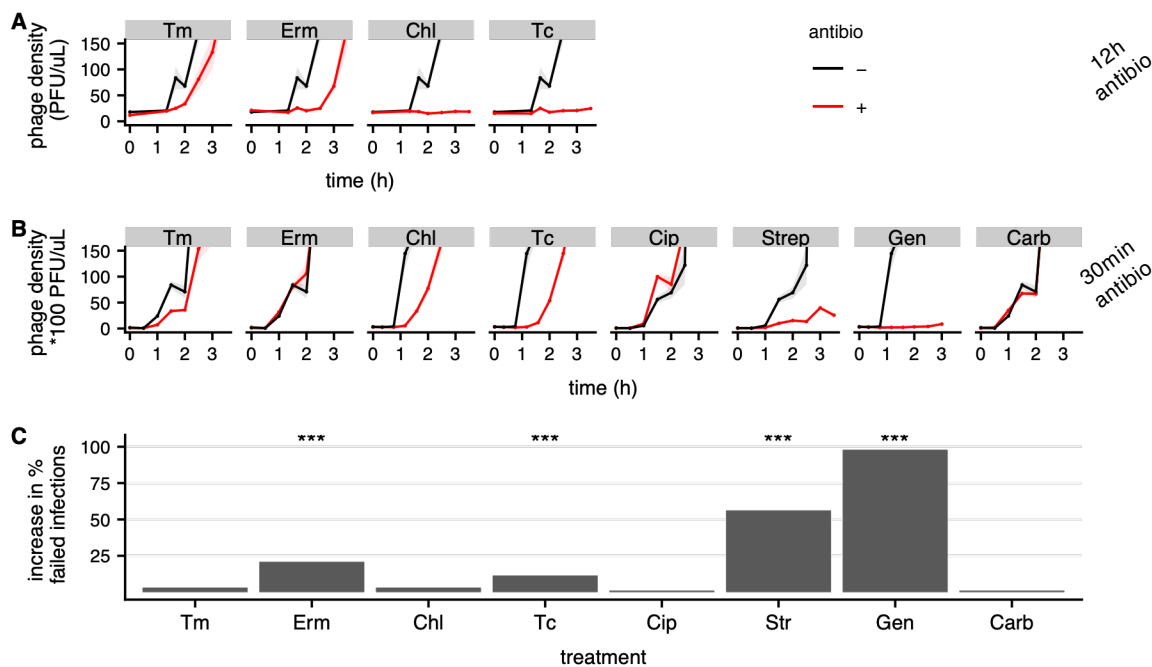
73

74 *Antibiotics effects on phage replication*

75 The common feature of bacteriostatic antibiotics is that they inhibit cell growth, which might
76 lead to higher rates of spacer acquisition¹⁴. To better understand the relationship between
77 bacterial growth and evolution of CRISPR immunity, we first measured bacterial growth
78 curves (based on the optical density, OD600, of the cultures) in the presence of each antibiotic
79 at concentrations used in our evolution experiments. Analysis of exponential growth rates in
80 batch culture and doubling times of individual cells in a microfluidics device¹⁵⁻¹⁷ showed that
81 Chl and Tc cause particularly slow growth and this is associated with a large increase in the
82 evolution of CRISPR-Cas immunity (Extended Data Fig. 4). More generally, this analysis
83 revealed a correlation between exponential growth rate and the evolution of CRISPR
84 immunity, with the exception of Erm, which was found to affect bacterial growth at higher cell
85 densities that are closer to stationary phase.

86 Bacteriostatic and bactericidal antibiotics impact cell metabolism differently, and lead
87 respectively to decreased and increased cell metabolic rates¹⁸. Because phage production is
88 dependent on the metabolism and protein synthesis machinery of the host^{19,20}, we hypothesized
89 that bacteriostatic antibiotics may slow down phage replication, which could provide a larger
90 window of time for the CRISPR-Cas immune system to acquire spacers from the phage prior
91 to irreversible cell damage or cell death. To test this hypothesis, we performed one-step phage
92 growth assays to detect when mature intracellular phages are produced. First, we pre-cultured
93 cells for 12 hours in the presence of each antibiotic, so that cells were close to stationary phase
94 and to the peak of phage epidemics in the absence of antibiotics. We found that all bacteriostatic
95 antibiotics caused a strong delay in phage production compared to cells cultured in the absence
96 of antibiotics (Fig. 2A). Under those conditions, we were unable to analyse the effect of
97 bactericidal antibiotics on phage production, due to high rates of cell death in these treatments.
98 Interestingly, when we next analysed the effects of antibiotics during exponential growth, we

99 found that Erm had no effect on phage production (Fig 2B), consistent with its minor effect on
100 exponential growth rate of the bacteria (Extended Data Fig. 4). All other bacteriostatic
101 antibiotics (Chl, Tc and Tm) delayed the formation of infectious progeny phages (Fig. 2B), and
102 this effect was observed across a broad range of Chl concentrations (Extended Data Fig. 3B).
103 These data strongly suggest that inhibition of bacterial growth by bacteriostatic antibiotics
104 causes a delay in the phage eclipse period. Bactericidal antibiotic had more variable effects:
105 Cip and Carb showed no interference with production of infectious phages, in agreement with
106 their mechanism of action and known synergy with phage therapy²¹, whereas the presence of
107 Strep or Gen (both aminoglycosides) resulted in very little phage production (Fig. 2B) due to
108 a large proportion of unproductive infections (Fig. 2C). Interestingly, we also observed a small
109 but significant increase in failed infections in the presence of Erm and Tc. While this may
110 contribute to the evolution of CRISPR immunity²², it is insufficient to explain the effects of
111 bacteriostatic antibiotics in general, since these had only small (Erm and Tc) or no effects (Tm,
112 Chl) on the proportion of unproductive infections (Fig. 2C).



113

114 **Figure 2: Bacteriostatic antibiotics delay production of mature phage particles.** A and B:
115 Effect of antibiotics on phage production dynamics. Phage density over time during infection
116 of cells that are pre-exposed to antibiotics for 12h (A) or 30min (B) are shown in red and no-
117 antibiotic controls in black. Lines and shaded areas are respectively mean and s.e.m. (N=4). C:
118 Effect of antibiotics on the frequency of failed phage infections. Barplots show the increase in
119 percentage of infected populations in which no phage was detected after 24h. Asterisks indicate
120 antibiotics with a significant increase in the number of populations with no phages (chi-square
121 tests, *** $p<0.001$).

122

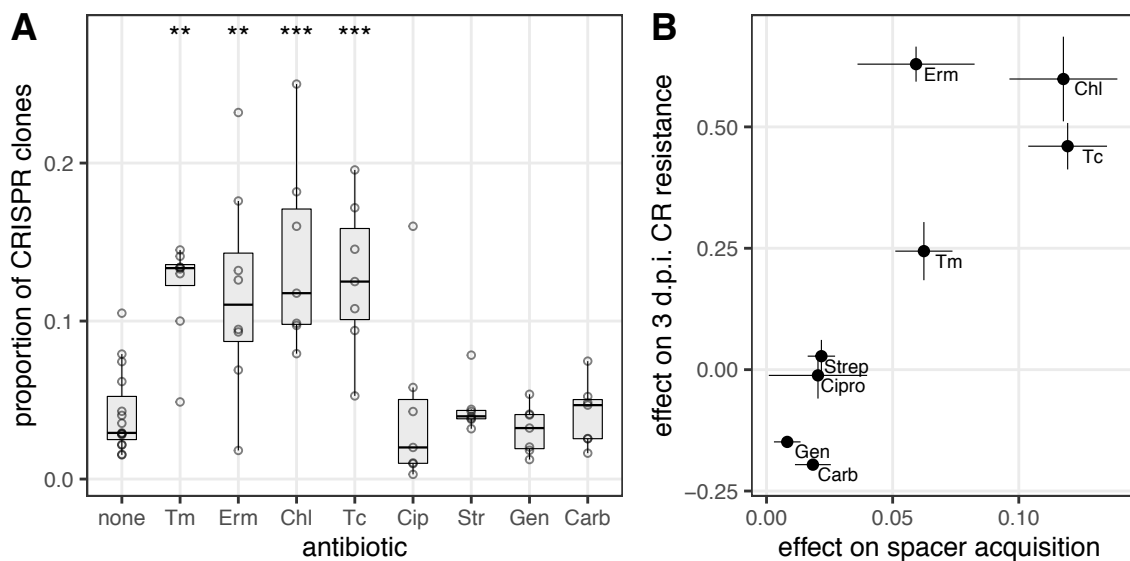
123 *Antibiotics effects on spacer acquisition*

124 We hypothesized that the reduced rate of within-host replication of phage in the presence of
125 bacteriostatic antibiotics may provide more time for infected cells to acquire CRISPR-Cas
126 immunity (i.e. to insert phage-derived spacers into CRISPR loci on the bacterial genome). To
127 test this hypothesis, we performed short-term (3h) infection assays and measured the
128 proportion of bacteria that had acquired new spacers in the presence or absence of each
129 antibiotic. This revealed that in the presence of all bacteriostatic antibiotics more cells acquire
130 CRISPR-Cas immunity, whereas bactericidal antibiotics had no effect (Fig. 3A). This effect
131 was detectable despite bacteriostatic antibiotics inhibiting absolute cell growth (Extended Data
132 Fig. 5). Across antibiotics, the rate at which CRISPR immunity is acquired in these short-term
133 experiments was significantly correlated to the levels of CRISPR-Cas immunity that evolved
134 at 3 days post infection (Fig. 3B, Pearson's correlation $t_{1,6}=3.9$, $p=0.008$, $\rho=0.85$). Crucially,
135 none of the antibiotics except Cip affected the rates at which bacteria with SM are generated
136 (Extended Data Fig. 6). Furthermore, none of the antibiotics caused an increase in Cas protein
137 production (Extended Data Fig. 7). Finally, we also tested whether antibiotics impact the way
138 selection acts on clones with CRISPR immunity and receptor mutants. For example, CRISPR

139 immunity may be more effective (and therefore provide a greater fitness advantage) when
140 phage replicates more slowly. However, competition experiments between a clone with
141 CRISPR-Cas immunity (CR) and a SM-resistant clone showed that the presence of
142 bacteriostatic antibiotics had either no impact or reduced the fitness of CRISPR immune
143 bacteria relative to receptor mutants (Extended Data Fig. 8). Collectively, these data therefore
144 show that bacteriostatic antibiotics increase the frequency at which cells survive phage
145 infection as a result of the acquisition of CRISPR-Cas immunity when phage replicate more
146 slowly. Consistent with this conclusion, the bacteriostatic antibiotic Chl only triggered
147 increased evolution of CRISPR immunity if it was present during the first day following phage
148 infection (Extended Data Fig. 9), when most cells are still phage-sensitive (Extended Data Fig.
149 2C), and later exposure, when bacteria have already acquired resistance, had no effect.

150

151



152

153 **Figure 3: Bacteriostatic antibiotics increase acquisition of CRISPR immunity.** A shows
154 the proportion of resistant clones which are CRISPR-Cas immune after 3h phage infection. The
155 centre value of the boxplots, boxes and whiskers respectively represent the median, first and
156 third quartile, and 1.5 times the interquartile range; dots show individual data points (N=6).

157 Asterisks show treatments significantly different from the no-antibiotic control (Tukey HSD;
158 **, $0.001 < p < 0.01$; ***, $p < 0.001$). In B, the average change in proportion per treatment is
159 plotted against the average increase in proportion of CRISPR-Cas immune clones in the
160 evolution experiments shown in Fig. 1, error bars showing s.e.m. (N=6).

161

162 ***Poor nutrients also promote CRISPR-Cas***

163 Given that bacteriostatic antibiotics promote the evolution of CRISPR immune bacteria, we
164 hypothesized that other environmental factors that slow down bacterial growth rate could also
165 lead to an increase in the evolution of CRISPR immunity. To test this hypothesis, we performed
166 evolution experiments in minimal medium with different carbon sources (glycerol, glucose and
167 pyruvate), which are associated with different maximum growth rates (Extended Data Fig.
168 10A). One-step growth curves in these different media showed that phage production was
169 delayed when cells grew on the poorest carbon source, glycerol (Extended Data Fig. 10B), as
170 expected based on changes in cell metabolic rates^{20,23,24}. Infection experiments at two different
171 phage inoculum sizes, which maximizes the dynamic range of any changes in the evolution of
172 CRISPR-Cas immunity¹³, showed that carbon source had a significant effect on the proportion
173 of bacteria that acquired CRISPR-Cas immunity (Extended Data Fig. 10C, $F_{2,32}=16.8$, $p=10^{-5}$).
174 Specifically, cells growing on glycerol grew more slowly and acquired CRISPR-Cas immunity
175 more frequently than those growing on glucose (Tukey HSD, $p=0.038$), whereas cells growing
176 on pyruvate grew more rapidly and acquired CRISPR-Cas immunity less frequently (Tukey
177 HSD, $p=0.008$). This was not due to differences in overall phage production¹³ (Extended Data
178 Fig. 10D and E) and therefore suggests that bacterial growth rate is a key determinant of the
179 frequency at which bacteria acquire CRISPR-Cas immunity.

180

181 ***Discussion***

182 Phage therapy can benefit patients by killing bacteria and by exploiting trade-offs between
183 phage resistance and pathogen virulence²⁵ or antibiotic resistance^{2,26}. However, *P. aeruginosa*
184 clones that acquire CRISPR-Cas immunity can escape these trade-offs and retain virulence⁷.
185 Previous studies have identified a number of environmental variables that shape the evolution
186 of CRISPR immunity by affecting the fitness of CRISPR-Cas immune *P. aeruginosa* clones
187 relative to those with mutated phage receptors^{7,13,27}. Here, we identify clinically relevant
188 environmental factors which increase the frequency at which sensitive *P. aeruginosa* clones
189 acquire CRISPR immunity during a phage infection. Acquisition of CRISPR-Cas immunity
190 relies on the acquisition of spacers from infecting phages, subsequent expression of appropriate
191 protective CRISPR RNAs and interference. It is a major limiting step because cells that just
192 acquired spacers might still be killed before mounting a sufficient immune response^{5,28}. We
193 found that bacteriostatic antibiotics promote the acquisition of CRISPR-Cas immunity over a
194 large range of concentrations, due to slowing bacterial growth, which in turn delays phage
195 development. This is consistent with increased spacer acquisition from plasmids under
196 conditions that are associated with slow bacterial growth^{14,29}. Interestingly, a number of
197 CRISPR-Cas systems have recently been found to induce dormancy following target
198 recognition³⁰⁻³² or to be coupled to genes that induce dormancy^{33,34}. A dormancy response of
199 infected cells with CRISPR immunity can benefit neighbouring cells by eliminating phage
200 from the environment and by limiting the invasion of phage mutants that overcome CRISPR
201 immunity³¹. Our data suggest the possibility that another advantage of a dormancy response
202 could be that they may lead to more efficient spacer acquisition during infections. Our findings
203 may also help to explain why the acquisition of CRISPR-Cas immunity is relatively rare under
204 laboratory conditions, in which bacteria commonly grow at rates much higher than in the
205 wild³⁵, and in clinical contexts. *Pseudomonas aeruginosa* displays slow growth rates in
206 biofilms³⁶ and in cystic fibrosis³⁷, which will be compounded by antimicrobial treatment. Our

207 results suggest that phage-antibiotic combination therapy should consider the possibility of
208 increased evolution of CRISPR immunity.

209

210 **Methods**

211 No statistical methods were used to pre- determine sample size. The experiments were not
212 randomized, and investigators were not blinded to allocation during experiments and outcome
213 assessment.

214

215 **Bacteria, phages and growth conditions**

216 Except when stated otherwise, evolution experiments and phage assays used *P. aeruginosa*
217 UCBPP-PA14 (PA14) and lytic phage DMS3vir¹¹. UCBPP-PA14 *csy3::lacZ* was used for
218 phage stock amplification, phage titre determination and estimation of Cas protein expression.
219 Competition experiments used a surface mutant (3A) derived from PA14 *csy3::lacZ* and a
220 CRISPR-resistant mutant (BIM4, bacteriophage insensitive mutant with 2 additional acquired
221 spacers against DMS3vir) derived from PA14, both of which have been previously described³⁸.
222 DMS3vir and a mutant expressing anti-CRISPR against PA14 IF system, DMS3vir *AcrIF1*,
223 were used for determination of resistance phenotypes¹³. Evolution experiments in the presence
224 of Chl also used PA14-*cat*, a Chl-resistant mutant of PA14 carrying the *cat* gene inserted into
225 the genome using a variant of plasmid pBAM³⁹ carrying *cat*. To this end, the *cat* gene was
226 amplified from plasmid pKD3⁴⁰ using primers
227 TAGATTAAATGATCGGCACGTAAGAGGTT and
228 CTGACCCTTGTCTTACGCCCGCCCTGCCACT, then ligated into pBAM1 after digestion
229 with SwaI and PshAI. For microfluidics experiments, we used PA14 *flgK::Tn5B30(Tc^R)*⁴¹.
230 All bacterial strains were grown at 37 °C in LB broth or M9 medium (22 mM Na₂HPO₄; 22
231 mM KH₂PO₄; 8.6 mM NaCl; 20 mM NH₄Cl; 1 mM MgSO₄; and 0.1 mM CaCl₂) supplemented

232 with 40 mM glucose, glycerol or pyruvate. All liquid cultures were grown with 180 rpm
233 shaking. For experiments using M9, overnight pre-cultures were themselves grown in M9 with
234 the same carbon source.

235

236 Determination of antibiotic activity

237 For MIC (minimum inhibitory concentration) determination, overnight cultures ($\sim 5 \cdot 10^9$ cells
238 /mL) were diluted 10⁴-fold in LB medium. 20 μ L of the diluted cultures were inoculated into
239 96-well microplate wells containing 180 μ L of LB supplemented with antibiotics using 2-fold
240 serial dilutions of the antibiotic. After 18 h growth at 37 °C, MIC was determined as the lowest
241 antibiotic concentration with no visible growth. To determine the MBC (minimal bactericidal
242 concentration), the content of wells with no visible growth was plated on LB-agar and further
243 incubated overnight. MBC was defined as the lowest antibiotic concentration resulting in
244 99.9% decrease in initial inoculum cell density (< 5 CFU in 100 μ L). MBC/MIC ratio was
245 used to estimate if antibiotic activity was bacteriostatic or bactericidal: a high MBC/MIC ratio
246 indicates that the concentration sufficient to prevent growth is much lower than the
247 concentration required to kill the majority of cells⁴². In our assay, antibiotics with average
248 MBC/MIC ratio >1 were the ones that are commonly recognized as being bacteriostatic (Tm,
249 Erm, Chl and Tc).

250

251 Evolution experiments

252 Evolution experiments were performed in glass vials containing 6 mL growth medium and
253 appropriate antibiotics at the concentrations shown in Extended Data Fig. 1. 60 μ L from
254 overnight cultures were co-inoculated with 10⁴ plaque-forming units (p.f.u.) of phage
255 DMS3vir, with the exception of the experiment in Extended Data Fig. 10, where two different
256 phage inocula of 10⁴ and 10⁹ p.f.u. were used. 1:100 volume was then transferred every 24 h

257 into fresh medium for 3 days with the exception of the experiment in Extended Data Fig. 10,
258 which was carried out for 5 days. Each treatment contained 6 biological replicates. Cell
259 densities and phage titers were monitored daily with serial dilution in M9 salts (after
260 chloroform treatment for phages), and enumeration of colonies on LB-agar and enumeration
261 of plaques on a lawn of PA14 *csy3::lacZ* cells. The identification of phage resistance type
262 (sensitive, CRISPR-Cas or SM) was performed by cross-streaking 24 randomly selected
263 colonies on DMS3vir and DMS3vir-AcrF1 phages: SM clones are resistant to both phages and
264 have a characteristic smooth colony morphology, whereas clones with CRISPR-Cas immunity
265 are resistant to DMS3vir but sensitive to DMS3vir-AcrF1¹³.

266

267 Determination of bacterial growth rate by optical density

268 Overnight cultures were diluted 100-fold into fresh growth media. Growth of 200 μ L of culture
269 was measured in a 96-well plate by measuring optical density at $\lambda=600\text{nm}$ (OD600) for 14 to
270 24 h at 37 °C in a BioTek Synergy 2 Plate reader, with 5 s shaking before each measurement.
271 All growth curves were performed in at least 8 replicates. Exponential growth rate was
272 determined in R using the package growthrates⁴³.

273

274 Determination of bacterial doubling time by microfluidics

275 The mother machine device was fabricated and handled as previously reported^{15,16}. Briefly,
276 overnight cultures in LB were spun down via centrifugation for 5 minutes at 4000 rpm at room
277 temperature (Eppendorf 5810 R). The supernatant was filtered twice (Medical Millex-GS
278 Filter, 0.22 μm , Millipore Corp.) and used to re-suspend the bacteria to an OD600 of 75. 2 μl
279 of the bacterial suspension was injected into the microfluidic mother machine device and
280 incubated at 37 °C until there were 1-2 bacteria in the lateral side channels. Fluorinated
281 ethylene propylene tubing (1/32" \times 0.008") was connected to the inlet and outlet holes and

282 connected to a computerized pressure-based flow control system (MFCS-4C, Fluigent)
283 controlled by MAESFLO software (Fluigent) and outlet reservoir respectively. Spent media
284 was flushed through the device to wash excess bacteria out of the main channel at 300 μ L/h
285 for 8 minutes to completely exchange the fluid in the device and tubing. The chip was mounted
286 on an inverted microscope (IX73 Olympus, Tokyo, Japan) and images were acquired in bright-
287 field via a 60 \times , 1.2 N.A. objective (UPLSAPO60XW, Olympus) and a sCMOS camera (Zyla
288 4.2, Andor, Belfast, UK) with a 0.03s exposure. The microfluidic device was moved by two
289 automated stages (M- 545.USC and P-545.3C7, Physik Instrumente, Karlsruhe, Germany, for
290 coarse and fine movements, respectively) to image multiple fields of view in a sequential
291 manner. The imaging setup was controlled by LabView. After acquiring the first set of images,
292 we flowed each of the investigated antibiotics dissolved in LB at the appropriate concentration
293 at 300 μ L/h for 8 minutes before lowering the flow rate to 100 μ L/h for 3 hours. The entire
294 assay was carried out at 37 °C in an environmental chamber surrounding the microscope.
295 Bacterial doubling times were extracted from the acquired image sets as previously reported¹⁷.
296 Briefly, we tracked each individual bacterium and its progeny throughout each experiment and
297 doubling times were measured as the lapses of time between successive bacterial divisions that
298 were assessed by eye through the images loaded in ImageJ and considered to have happened
299 when two daughter cells became clearly distinguishable from their respective parental cell.
300

301 One-step phage growth assays

302 Overnight cultures of PA14 were first diluted into 6 mL growth medium \pm antibiotic treatment
303 in glass vials (N=4). For experiments with 30 min of pre-exposure to antibiotics, cells were
304 diluted 25-fold into fresh media with antibiotics and grown for 30 min before phage addition.
305 For experiments with 12 h of pre-exposure to antibiotics, cells were diluted 100-fold into fresh
306 media with antibiotics and grown for 12 h before phage addition. Bactericidal treatments were

307 excluded from further analysis because they caused a 4-fold to 570-fold decrease in cell density
308 after 12 h, making it impossible to determine the latent period of phage under those conditions.
309 After growing in the presence of antibiotics, approximately 5.10^7 p.f.u. of DMS3vir were added
310 in each vial, and vials were vortexed and incubated at 37 °C for 15 min, allowing phage
311 adsorption. Cultures were then diluted 1000-fold into 6 mL growth medium ± antibiotic
312 treatment to limit further adsorption and re-infection, vortexed again and transferred to 24-well
313 plates for parallel processing. Samples were taken immediately (t=0) and then approximately
314 every 20 minutes. The first samples were diluted in M9 salts and plated on LB-agar to quantify
315 cell densities; all samples were chloroform-treated and plated on PA14 *csy3::lacZ* lawns.
316 Phage densities measured after chloroform treatment correspond to the sum of free phages and
317 mature phage particles inside infected cells.

318

319 Determination of antibiotic effects on infection success

320 Four overnight cultures of PA14 were diluted in parallel 100-fold into LB with or without
321 antibiotics. After 2 h growth at 37 °C, DMS3vir phages were added to a final concentration of
322 1000 p.f.u./mL (equivalent to 5 p.f.u. in 200 µL) and the vials were vortexed. After 15 min at
323 37 °C, vials were vortexed again and 24* 200 µL of each individual culture were aliquoted into
324 24 wells of a 96-well plate. Plates were incubated at 37 °C for 22 h, then 20 µL of each well
325 were spotted on a lawn of PA14 *csy3::lacZ* cells in two replicates. With an average phage
326 inoculum of 5 phages, the distribution of phages across wells is expected to follow a Poisson
327 distribution with 0.7% wells containing 0 phages and 1.3% wells containing more than 10
328 phages. The control treatment with no antibiotics was consistent with this, as 1 in 96 wells
329 produced no lysis. Lysis indicated that the founding phages reproduced. The number of wells
330 in which phages failed to reproduce was counted for each treatment, and significance was
331 determined by chi-square tests between antibiotic and no-antibiotic treatment.

332

333 Measurement of mutation towards SM

334 To evaluate the frequency of SM cells in the absence of phage selection, cells were grown in
335 LB ± antibiotic treatment for 24 h. After 24 h, cultures were serially diluted in M9 salts, then
336 dilutions were plated both on LB-agar to calculate total cell density, and on LB-agar containing
337 a high concentration of DMS3vir, which was generated by covering the agar surface with a
338 phage stock of 10^8 p.f.u./ μ L. The density of SM mutants was calculated from counting the
339 number of colonies growing on top of DMS3vir. Three independent experiments were run with
340 6 experimental replicates each.

341

342 Spacer acquisition assay

343 20 μ L of PA14 overnight culture were first diluted 1:50 into 1 mL LB with or without
344 antibiotics in 24-well plates, in 8 replicates per treatment. After 30 min of growth at 37 °C,
345 2.10^9 DMS3vir phages were added per well, and cultures were incubated at 37 °C for 3h. The
346 density of phage-sensitive cells was measured by plating 100 μ L on LB-agar after 10^4 -fold
347 dilution in M9 salts. The density of phage-resistant cells was measured by directly plating 100
348 μ L of cultures on LB-agar without dilution: the phage density on these plates was sufficient to
349 prevent growth of sensitive colonies. The majority of colonies had a smooth morphology
350 characteristic of SM clones. We confirmed that smooth colonies were resistant to both
351 DMS3vir and DMS3vir+AcrIF1, whereas non-smooth colonies were resistant to DMS3vir but
352 sensitive to DMS3vir+AcrIF1, and were therefore CRISPR immune. In each culture, the
353 proportion of CRISPR-Cas immune clones within the total population of resistant clones
354 (CRISPR-Cas and SM) was calculated.

355

356 Competition assays

357 Competition experiments were performed in 6 mL LB supplemented in the presence or absence
358 of antibiotics. They were initiated by inoculating 60 μ L of a 1:1 mix of LB overnight cultures
359 of CRISPR-Cas immune (BIM2) and surface mutant (3A) clones. For treatments including
360 phages, 8.10⁹ p.f.u. DMS3vir were added per vial. Samples were serially diluted at 0 and 24 h
361 and plated on LB agar supplemented with 50 μ g/mL X-Gal, to determine the ratio of the surface
362 mutant that carries the *LacZ* gene and therefore forms blue colonies, and the BIM2, which
363 forms white colonies. The selection rate of the CRISPR-Cas clone was calculated as $m_{BIM2} -$
364 m_{3A} , with m the Malthusian parameter defined as $\log(\text{density}(t_1)/\text{density}(t_0))$ ⁴⁴. We used
365 selection rate rather than relative fitness because some treatments led to an absolute decline in
366 the abundance of the CRISPR-Cas clone.

367

368 Cas expression assay

369 We used PA14 *csy3::lacZ* as a reporter strain for Cas gene expression, using the β -
370 Galactosidase fluorogenic substrate 4-Methylumbelliferyl β -D-galactoside⁴⁵ (MUG). An
371 overnight culture of PA14 *csy3::lacZ* was diluted 100-fold into 6 mL of LB with or without
372 antibiotics. After 5 h of growth, OD600 was recorded and 100 μ L aliquots were immediately
373 frozen at -80 °C. Prior to the assay, the frozen 96-well plate was defrosted and 10 μ L were
374 transferred to a new plate and frozen again at -80 °C for 1 h. After transfer to 37 °C, 100 μ L
375 reagent solution (0.25 mg/mL MUG and 2 mg/mL lysozyme in phosphate-buffered saline) was
376 added to each well. Fluorescence was measured for 30 min in a Thermo Scientific Varioskan
377 flash plate reader at 37 °C, with excitation and emission wavelengths respectively 365 nm and
378 450 nm. The 15 min timepoint was used for analysis. Relative fluorescence was calculated as
379 (fluorescence at 15 min – fluorescence at 0 min) / OD600.

380

381 Statistics

382 All statistical analyses were done with R version 3.4.1⁴⁶, and package cowplot⁴⁷. Evolution
383 experiments with antibiotics were not all performed simultaneously (Figure 1, Extended Data
384 Fig. 1, Extended Data Fig. 3): for these, we used individual Student t-tests comparing each
385 treatment to the associated no-antibiotic treatment. For experiments in M9 that used two
386 different phage inocula (Extended Data Fig. 10), the effect of the two treatments was modelled
387 as: proportion of CRISPR-Cas immune clones ~ carbon source + phage inoculum.

388

389 **Acknowledgments**

390 This work was funded by grants from the European Research Council under the European
391 Union's Horizon 2020 research and innovation programme (ERC-2017-ADG-788405 to
392 M.D.S and ERC-STG-2016-714478 to E.R.W.) E.R.W. was further supported by a NERC
393 Independent Research Fellowship (NE/M018350/1).

394

395 **Author contributions**

396 Conceptualization of the study was done by T.D. and E.R.W. Experimental design was carried
397 out by T.D. Bacterial evolution, competition and growth experiments as well as phage infection
398 assays were done by T.D. with assistance from E.K., and MIC measurements were done by
399 E.K. Microfluidics experiments were designed and carried out by U.L. and S.P. Formal
400 analysis of results was done by T.D. K.S. and M.D.S. contributed to discussions and provided
401 feedback throughout the project. T.D. wrote the original draft of the manuscript, with later edits
402 and reviews by T.D., K.S., S.P., M.D.S. and E.R.W.

403

404 **Competing interests**

405 The authors declare no competing interests.

406

407 **References**

- 408 1. Segall, A. M., Roach, D. R. & Strathdee, S. A. Stronger together? Perspectives on phage-
409 antibiotic synergy in clinical applications of phage therapy. *Current Opinion in
410 Microbiology* **51**, 46–50 (2019).
- 411 2. Kortright, K. E., Chan, B. K., Koff, J. L. & Turner, P. E. Phage Therapy: A Renewed
412 Approach to Combat Antibiotic-Resistant Bacteria. *Cell Host & Microbe* **25**, 219–232
413 (2019).
- 414 3. Torres-Barceló, C. & Hochberg, M. E. Evolutionary Rationale for Phages as Complements
415 of Antibiotics. *Trends in Microbiology* **24**, 249–256 (2016).
- 416 4. Labrie, S. J., Samson, J. E. & Moineau, S. Bacteriophage resistance mechanisms. *Nature
417 Reviews Microbiology* **8**, 317–327 (2010).
- 418 5. Jackson, S. A. *et al.* CRISPR-Cas: Adapting to change. *Science* **356**, eaal5056 (2017).
- 419 6. Garneau, J. E. *et al.* The CRISPR/Cas bacterial immune system cleaves bacteriophage and
420 plasmid DNA. *Nature* **468**, 67–71 (2010).
- 421 7. Alseth, E. O. *et al.* Bacterial biodiversity drives the evolution of CRISPR-based phage
422 resistance. *Nature* **574**, 549–552 (2019).
- 423 8. De Smet, J., Hendrix, H., Blasdel, B. G., Danis-Wlodarczyk, K. & Lavigne, R.
424 Pseudomonas predators: understanding and exploiting phage–host interactions. *Nat Rev
425 Microbiol* **15**, 517–530 (2017).
- 426 9. Tagliaferri, T. L., Jansen, M. & Horz, H.-P. Fighting Pathogenic Bacteria on Two Fronts:
427 Phages and Antibiotics as Combined Strategy. *Front. Cell. Infect. Microbiol.* **9**, 22 (2019).
- 428 10. Torres-Barceló, C., Gurney, J., Gougam-Barberá, C., Vasse, M. & Hochberg, M. E.
429 Transient negative effects of antibiotics on phages do not jeopardise the advantages of
430 combination therapies. *FEMS Microbiology Ecology* **94**, (2018).

431 11. Cady, K. C., Bondy-Denomy, J., Heussler, G. E., Davidson, A. R. & O'Toole, G. A.
432 The CRISPR/Cas Adaptive Immune System of *Pseudomonas aeruginosa* Mediates
433 Resistance to Naturally Occurring and Engineered Phages. *Journal of Bacteriology* **194**,
434 5728–5738 (2012).

435 12. Barrangou, R. *et al.* CRISPR Provides Acquired Resistance Against Viruses in
436 Prokaryotes. *Science* **315**, 1709–1712 (2007).

437 13. Westra, E. R. *et al.* Parasite Exposure Drives Selective Evolution of Constitutive
438 versus Inducible Defense. *Current Biology* **25**, 1043–1049 (2015).

439 14. Høyland-Kroghsbo, N. M., Muñoz, K. A. & Bassler, B. L. Temperature, by
440 Controlling Growth Rate, Regulates CRISPR-Cas Activity in *Pseudomonas aeruginosa*.
441 *mBio* **9**, (2018).

442 15. Bamford, R. A. *et al.* Investigating the physiology of viable but non-culturable
443 bacteria by microfluidics and time-lapse microscopy. *BMC Biol* **15**, 121 (2017).

444 16. Cama, J. *et al.* Single-cell microfluidics facilitates the rapid quantification of
445 antibiotic accumulation in Gram-negative bacteria. *Lab Chip* **20**, 2765–2775 (2020).

446 17. Łapińska, U., Glover, G., Capilla-Lasheras, P., Young, A. J. & Pagliara, S. Bacterial
447 ageing in the absence of external stressors. *Phil. Trans. R. Soc. B* **374**, 20180442 (2019).

448 18. Lobritz, M. A. *et al.* Antibiotic efficacy is linked to bacterial cellular respiration.
449 *Proceedings of the National Academy of Sciences* **112**, 8173–8180 (2015).

450 19. Hadas, H., Einav, M., Fishov, I. & Zaritsky, A. Bacteriophage T4 Development
451 Depends on the Physiology of its Host *Escherichia Coli*. *Microbiology* **143**, 179–185
452 (1997).

453 20. You, L., Suthers, P. F. & Yin, J. Effects of *Escherichia coli* Physiology on Growth of
454 Phage T7 In Vivo and In Silico. *JB* **184**, 1888–1894 (2002).

455 21. Comeau, A. M., Tetart, F., Trojet, S. N., Prere, M.-F. & Krisch, H. M. Phage-
456 Antibiotic Synergy (PAS): β -Lactam and Quinolone Antibiotics Stimulate Virulent Phage
457 Growth. *PLoS ONE* **4** (2007).

458 22. Hynes, A. P., Villion, M. & Moineau, S. Adaptation in bacterial CRISPR-Cas
459 immunity can be driven by defective phages. *Nature Communications* **5**, 4399 (2014).

460 23. Rabinovitch, A., Fishov, I., Hadas, H., Einav, M. & Zaritsky, A. Bacteriophage T4
461 Development in *Escherichia coli* is Growth Rate Dependent. *Journal of Theoretical
462 Biology* **216**, 1–4 (2002).

463 24. Payne, P., Geyrhofer, L., Barton, N. H. & Bollback, J. P. CRISPR-based herd
464 immunity can limit phage epidemics in bacterial populations. *eLife* **7**, e32035 (2018).

465 25. León, M. & Bastías, R. Virulence reduction in bacteriophage resistant bacteria. *Front.
466 Microbiol.* **06**, (2015).

467 26. Chan, B. K. *et al.* Phage selection restores antibiotic sensitivity in MDR *Pseudomonas
468 aeruginosa*. *Scientific Reports* **6**, (2016).

469 27. van Houte, S. *et al.* The diversity-generating benefits of a prokaryotic adaptive
470 immune system. *Nature* **532**, 385–388 (2016).

471 28. Modell, J. W., Jiang, W. & Marraffini, L. A. CRISPR–Cas systems exploit viral DNA
472 injection to establish and maintain adaptive immunity. *Nature* **544**, 101–104 (2017).

473 29. Amlinger, L., Hoekzema, M., Wagner, E. G. H., Koskineni, S. & Lundgren, M.
474 Fluorescent CRISPR Adaptation Reporter for rapid quantification of spacer acquisition.
475 *Scientific Reports* **7**, (2017).

476 30. Rostøl, J. T. & Marraffini, L. A. Non-specific degradation of transcripts promotes
477 plasmid clearance during type III-A CRISPR–Cas immunity. *Nat Microbiol* **4**, 656–662
478 (2019).

479 31. Meeske, A. J., Nakandakari-Higa, S. & Marraffini, L. A. Cas13-induced cellular
480 dormancy prevents the rise of CRISPR-resistant bacteriophage. *Nature* **570**, 241–245
481 (2019).

482 32. Rostøl, J. T. *et al.* The Card1 nuclease provides defence during type III CRISPR
483 immunity. *Nature* **590**, 624–629 (2021).

484 33. Koonin, E. V. & Zhang, F. Coupling immunity and programmed cell suicide in
485 prokaryotes: Life-or-death choices. *BioEssays* **39**, e201600186 (2017).

486 34. Makarova, K. S., Anantharaman, V., Aravind, L. & Koonin, E. V. Live virus-free or
487 die: coupling of antivirus immunity and programmed suicide or dormancy in prokaryotes.
488 *Biol Direct* **7**, 40 (2012).

489 35. Gibson, B., Wilson, D. J., Feil, E. & Eyre-Walker, A. The distribution of bacterial
490 doubling times in the wild. *Proceedings of the Royal Society B: Biological Sciences* **285**, 9
491 (2018).

492 36. Werner, E. *et al.* Stratified Growth in *Pseudomonas aeruginosa* Biofilms. *AEM* **70**,
493 6188–6196 (2004).

494 37. Yang, L. *et al.* In Situ Growth Rates and Biofilm Development of *Pseudomonas*
495 *aeruginosa* Populations in Chronic Lung Infections. *JB* **190**, 2767–2776 (2008).

496 38. Cady, K. C. & O'Toole, G. A. Non-Identity-Mediated CRISPR-Bacteriophage
497 Interaction Mediated via the Csy and Cas3 Proteins. *Journal of Bacteriology* **193**, 3433–
498 3445 (2011).

499 39. Martínez-García, E., Calles, B., Arévalo-Rodríguez, M. & de Lorenzo, V. pBAM1: an
500 all-synthetic genetic tool for analysis and construction of complex bacterial phenotypes.
501 *BMC microbiology* **11**, 38 (2011).

502 40. Datsenko, K. A. & Wanner, B. L. One-step inactivation of chromosomal genes in
503 *Escherichia coli* K-12 using PCR products. *Proceedings of the National Academy of
504 Sciences* **97**, 6640–6645 (2000).

505 41. O'Toole, G. A. & Kolter, R. Flagellar and twitching motility are necessary for
506 *Pseudomonas aeruginosa* biofilm development. *Molecular Microbiology* **30**, 295–304
507 (1998).

508 42. Pankey, G. A. & Sabath, L. D. Clinical Relevance of Bacteriostatic versus
509 Bactericidal Mechanisms of Action in the Treatment of Gram-Positive Bacterial
510 Infections. *Clinical Infectious Diseases* **38**, 864–870 (2004).

511 43. Petzoldt, T. growthrates: Estimate Growth Rates from Experimental Data. R package
512 version 0.7.2. (2018).

513 44. Lenski, R. E., Rose, M. R., Simpson, S. C. & Tadler, S. C. Long-Term Experimental
514 Evolution in *Escherichia coli*. I. Adaptation and Divergence During 2,000 Generations.
515 *The American Naturalist* **138**, 1315–1341 (1991).

516 45. Ramsay, J. High-throughput β -galactosidase and β -glucuronidase Assays Using
517 Fluorogenic Substrates. *BIO-PROTOCOL* **3**, (2013).

518 46. R Core Team. R: A language and environment for statistical computing. *Vienna,
519 Austria*. (2017).

520 47. Wilke, C. O. *cowplot: Streamlined Plot Theme and Plot Annotations for 'ggplot2'*. R
521 package version 0.8.0. (2017).

522